

Photoelectron imaging of I_2^- at 5.826 eV

Bradley F. Parsons, Sean M. Sheehan, Kathryn E. Kautzman,
Terry A. Yen, and Daniel M. Neumark^{a)}

*Department of Chemistry, University of California at Berkeley, Berkeley, California 94720-1460
and Chemical Sciences Division, Lawrence Berkeley National Laboratory, Berkeley, California 94720*

(Received 25 August 2006; accepted 22 September 2006; published online 28 December 2006)

We report the anion photoelectron spectrum of I_2^- taken at 5.826 eV detachment energy using velocity mapped imaging. The photoelectron spectrum exhibits bands resulting from transitions to the bound regions of the $X^1\Sigma_g^+(0_g^+)$, $A'^3\Pi_u(2_u)$, $A^3\Pi_u(1_u)$, and $B^3\Pi_u(0_u^+)$ electronic states as well as bands resulting from transitions to the repulsive regions of several I_2 electronic states: the $B'^3\Pi_u(0_u^-)$, $B''^1\Pi_u(1_u)$, $^3\Pi_g(2_g)$, $a^3\Pi_g(1_g)$, $^3\Pi_g(0_g^-)$, and $C^3\Sigma_u^+(1_u)$ states. We simulate the photoelectron spectrum using literature parameters for the I_2^- and I_2 ground and excited states. The photoelectron spectrum includes bands resulting from transitions to several high-lying excited states of I_2 that have not been seen experimentally: $^3\Pi_g(0_g^-)$, $^1\Pi_g 3(1_g)$, $1^3\Sigma_g^- 3(0_g^+)$, and the $^1\Sigma_g^- 3(0_u^-)$ states of I_2 . Finally, the photoelectron spectrum at 5.826 eV allows for the correction of a previous misassignment for the vertical detachment energy of the $I_2 B^3\Pi_u(0_u^+)$ state. © 2006 American Institute of Physics. [DOI: 10.1063/1.2363990]

I. INTRODUCTION

Molecular iodine represents one of the benchmark systems of diatomic spectroscopy. It presents unique experimental and theoretical challenges owing to its large number of excited electronic states and the importance of relativistic effects in determining the properties of these states. While the ground state and several excited states of I_2 have been characterized in exquisite detail,^{1–10} other relatively low-lying excited states have not been characterized experimentally, some because they are not optically allowed in transitions from the ground state and others because optical excitation from the I_2 ground state ($R_e=2.666$ Å) accesses strongly repulsive, spectrally congested regions of the potential energy curves for these states, resulting in overlapped, structureless bands, from which the extraction of contributions from individual electronic transitions is challenging.

Here we report the anion photoelectron spectroscopy of I_2^- at 212.8 nm using velocity mapped imaging (VMI). The experiment accesses several high-lying excited states of I_2 that have not been previously observed. Photoelectron spectroscopy has more relaxed selection rules than optical spectroscopy. Moreover, since the equilibrium bond distance in the ground state of I_2^- , 3.205 Å,¹¹ is considerably longer than in the I_2 ground state, the excited states accessed are, in most cases, better separated and more gently sloping, facilitating their characterization.

Molecular iodine has ten valence electrons and the orbital occupancy can be represented as $\sigma_g^m \pi_u^n \pi_g^p \sigma_u^q$, with $m+n+p+q=10$. It is convenient to classify the electronic states of I_2 and I_2^- using the notation proposed by Mulliken,¹¹ in which each I_2 state is labeled $mnpq$. Hence, the orbital occupancy for ground state I_2 is $\sigma_g^2 \pi_u^4 \pi_g^4 \sigma_u^0$ or 2440, while

that for ground state I_2^- is 2441 since the orbital occupancy is $\sigma_g^2 \pi_u^4 \pi_g^4 \sigma_u^1$. This notation facilitates identification of the one-electron photodetachment transitions that dominate photoelectron spectroscopy.

The potential energy surfaces for I_2 have been investigated extensively using a variety of theoretical techniques. Recent calculations for the ground and excited states of I_2 have used multireference configuration interaction⁹ with several treatments including relativistic effects.^{2,3,12} The spin-orbit interaction in I_2 gives a total of 23 valence electronic states converging to the three $I(^2P_\Omega)+I(^2P_\Omega)$ asymptotes. To remain consistent with previous studies^{1–3} of I_2 we give Hund's case (c) designation for the electronic states in parentheses, so the ground state is $X^1\Sigma_g^+(0_g^+)$. Figure 1 shows the potential energy curves for a portion of ground state of I_2 as well as some of the excited states of I_2 correlating with both $I(^2P_{3/2})+I(^2P_{3/2})$ and $I(^2P_{3/2})+I(^2P_{1/2})$ products. The I_2 potential energy curves are taken from Ref. 3. The vertical arrow and blue horizontal line denote the energetic limit for photodetachment from I_2^- using a 5.826 eV photon. The figure caption identifies the excited states of I_2 that are important in the present work.

The photoelectron spectroscopy of I_2^- has been studied using both conventional^{11,13} and ultrafast methods.^{11,14–16} Previous work from our group¹¹ used a combination of conventional and ultrafast anion photoelectron spectroscopy to develop a ground state Morse potential for I_2^- . Conventional anion photoelectron (PE) spectroscopy experiments have previously explored photodetachment transitions to the ground state of I_2 and the excited $A'^3\Pi_u(2_u)$ and $A^3\Pi_u(1_u)$ states at 299 nm.¹¹ Subsequent PE spectra at 266 nm (4.661 eV) showed transitions assigned to the $B'^3\Pi_u(0_u^-)$, $B''^1\Pi_u(1_u)$, and $B^3\Pi_u(0_u^+)$ states of I_2 , but did not confirm these assignments through simulations.¹³ As discussed below, the assignment of a peak at 4.418 eV binding energy to the $B^3\Pi_u(0_u^+)$ state of I_2 is in error; the current work corrects

^{a)} Author to whom correspondence should be addressed. Electronic mail: dneumark@berkeley.edu

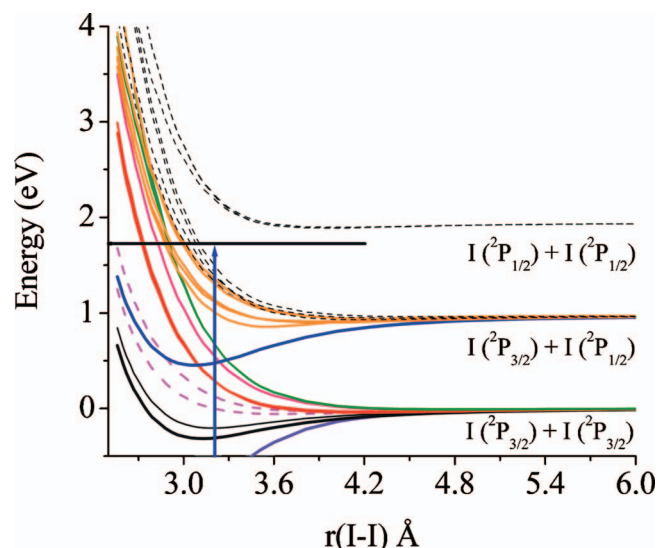


FIG. 1. (Color) The excited state potential energy surfaces of I_2 . The thick solid purple line is the $X^1\Sigma_g^+(0_g^+)$ ground state of I_2 . The A' $^3\Pi_u(2_u)$ appears as the thick black line and the A $^3\Pi_u(1_u)$ state at the thin black line. The B' $^3\Pi_u(0_u^-)$ and B'' $^1\Pi_u(1_u)$ states appear as the dashed magenta lines. The $^3\Pi_g(1_g)$ and the a $^3\Pi_g(1_g)$ excited states lie close in energy and appear as the red lines. The thick blue line is the B $^3\Pi_u(0_u^+)$ state. The solid pink line is the a' $^3\Pi_g(0_g^+)$. The olive line is two close lying excited states, namely, the 1 $^3\Sigma_u^+2(0_u^-)$ and the $^3\Delta_u(3_u)$ states. Finally, the series of states that contribute to band C are shown in orange. In order of increasing energy, these states are the $3(0_g^+)$, the $^3\Pi_g(0_g^-)$, the $^1\Pi_g3(1_g)$, the $3(0_u^-)$, and the C $^3\Sigma_u^+(1_u)$. The dashed black states correspond with I_2 states that are observed in the photoelectron spectrum.

the assignment and characterizes several higher electronic states by measuring the I_2^- photoelectron spectrum at 5.826 eV (212.8 nm) with VMI.

Anion photoelectron spectroscopy using VMI has become increasingly attractive as it offers high collection efficiency, reasonable resolution, and the ability to measure photoelectron kinetic energy and angular distributions simultaneously.^{16–19} Moreover, VMI is very sensitive to very low energy photoelectrons, in contrast to detection schemes based on field-free^{20,21} and magnetic bottle time-of-flight analyzers.²² However, the photoelectron imaging optics used to collect electrons are susceptible to production of background electrons from stray photons impinging on the optics. As a result, no anion VMI spectra have been reported at photon energies above 4.661 eV. We have made some simple

modifications to the electron optics that have resulted in significant reduction of background photoelectrons, enabling us to obtain VMI spectra at 5.826 eV and opening the possibility for future studies at higher photon energy.

In the next section, we review the essential components of our spectrometer and the required modifications to perform VMI at 5.826 eV. In Sec. III, results are presented along with a preliminary assignment of the individual bands in the PE spectrum. In Sec. IV, we discuss the fits to the bands in our photoelectron experiments by simulating photodetachment transitions to both neutral bound and unbound states.

II. EXPERIMENT

As with previous experiments, 15 psig Ar carrier gas passes over solid I_2 ; the resulting I_2 :Ar gas is expanded supersonically through a piezoelectric valve²³ and then crossed with a 1 keV electron beam. Anions are mass selected using a linear reflectron mass spectrometer giving a mass resolution of $m/\Delta m=2000$.

Anions are photodetached using 212.8 nm photons from the fifth harmonic of an Nd:YAG laser (SpectraPhysics PRO-290). The laser is focused 1.5 cm before the interaction region using a 50 cm fused silica lens and detached photoelectrons are collected using VMI.^{24,25} Conventional velocity mapped imaging^{24,25} uses a three plate ion optical stack to create an immersion lens in the interaction region of the chamber. As shown in Fig. 2(a), a laser crosses the neutral or anion species of interest perpendicular to the VMI time-of-flight axis [the vertical axis in Fig. 2(a)]. The lower plate (repeller) in the ion optics stack is typically solid or has a very small center hole (~ 1 –2 mm). The other two plates (extractor and ground) in the VMI stack have large center holes ($< 1/4$ of the outer diameter of the plate).

Figure 2(b) shows the experimental setup used in the current study. It incorporates two modifications aimed at reducing background electrons from photons striking the repeller. The repeller is equipped with a center grid [B in Fig. 2(b)], which allows for transmission of $\sim 70\%$ of all scattered photons while maintaining a uniform electric field in the interaction region. Below the repeller is an additional plate [A in Fig. 2(b)], which is maintained at a positive bias

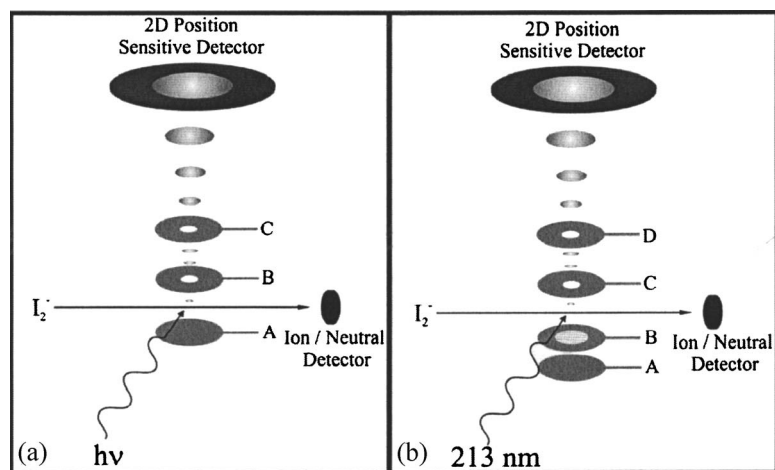


FIG. 2. (a) Experimental setup for traditional velocity mapped imaging. In traditional VMI, the anion beam and laser enter the interaction region perpendicular to the VMI time-of-flight axis. The imaging optics stack consists of three plates: repeller (A), extractor (B), and ground (C). (b) The experimental setup for the VMI detection used in these experiments. The 212.8 nm laser crosses the anion beam perpendicular to the VMI flight axis. The repeller (B) is fitted with a grid that allows for transmission of scattered laser photons. The solid plate (A) below the grid is maintained at a positive voltage to collect electrons scattered from the repeller.

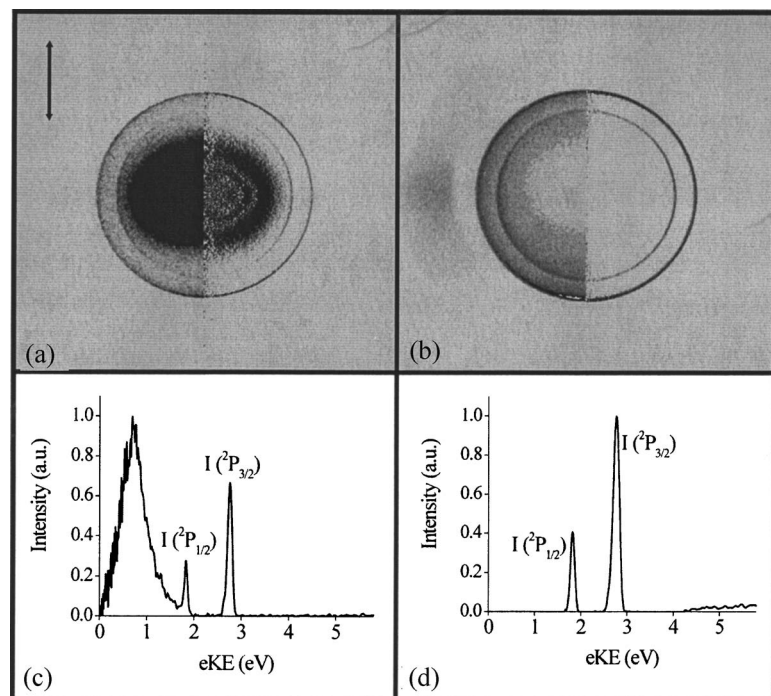


FIG. 3. Photoelectron images for I^- detached at 212.8 nm. The arrow shows the detachment laser polarization vector. (a) Photoelectron image (left half) and transformed image (right half) of I^- at 212.8 nm using traditional VMI imaging optics shown in (a) and (b). Photoelectron image (left half) and transformed image (right half) of I^- at 212.8 nm using the VMI imaging optics shown in (b). (c) Electron kinetic energy (eKE) distribution determined from the image in Fig. 4(a). The background from scattered laser photons gives an intense peak at low eKE. (d) Electron kinetic energy (eKE) distribution determined from the image in Fig. 4(b). The background from scattered laser photons gives a broad peak at high eKE.

during the experiment. The lower plate serves as an electron collector to remove background electrons ejected from the grid. Typical operating voltages are $A=3.0$ kV, $B=-1.7$ kV, $C=-1.1$ kV, and $D=0$ V.

With both arrangements, the laser and anion beam enter the interaction region perpendicular to the VMI time-of-flight axis. Neutrals formed by the detachment process are detected using a microchannel plate detector (MCP) positioned after the VMI region. Detached electrons are projected upwards towards a two dimensional (2D) position sensitive detector. The 2D detector consists of two microchannel plates and a phosphor screen. The phosphor screen output is imaged using a charge-coupled device (CCD) camera. To obtain the photoelectron spectrum, we perform an inverse Abel transform on the raw image using the basis set expansion (BASEX) program.²⁶ The photoelectron spectrum is calibrated by taking the photoelectron spectrum of I^- and Br^- at 212.8 nm. The full width at half maximum (FWHM) for the transition to the $I^2P_{3/2}$ state is ~ 2.0 pixels and the corresponding energy resolution is 2.5%.

Figure 3(a) shows the image of I^- photodetached at 212.8 nm using the conventional VMI imaging optical setup in Fig. 2(a). The bright spot dominating the center of the image is from background electrons ejected by laser photons striking the lower electron optic in the VMI stack. Figure 3(c) shows the photoelectron spectrum derived from the image in Fig. 3(a). The background electrons result in a peak at low electron kinetic energy (eKE), somewhat akin to what is seen in time-of-flight analyzers at the same or higher photon energy. Figure 3(b) shows the photoelectron image of I^- photodetached at 212.8 nm using the modified VMI optics shown in Fig. 2(b). The center spot is now gone, and instead one observes background electrons primarily as a spot to the left of the main image, presumably resulting from stray photons striking the solid outer ring of the repeller. Figure 3(d) shows the corresponding photoelectron spectrum. The back-

ground is much reduced in magnitude and appears at high electron kinetic energy. Electrons scattered from the grid are not velocity mapped onto the detector. Since the detachment laser is focused before the interaction region then most scattered electrons appear after the interaction region and map to the left side of the image in Fig. 3(b). This apparent shifting of the background to high eKE is desirable because the low eKE range is typically of greater interest at high photon energies.

III. RESULTS

Figure 4 shows the background subtracted velocity mapped image for photoelectrons detached from I_2^- at 212.8 nm along with the transformed image. Fluctuations in laser power, due to the unheated fifth harmonic crystal, result in the residual background spot to the left in Fig. 4. Figure 5

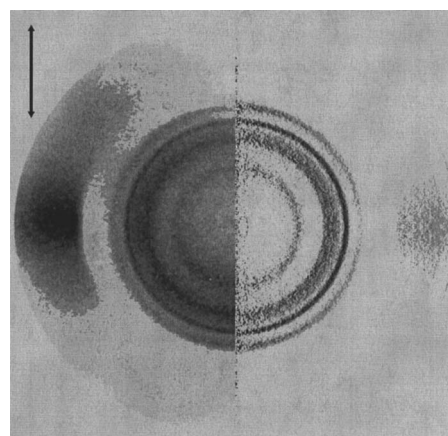


FIG. 4. Photoelectron image (left half) and the transformed image (right half) for I_2^- detached at 5.826 eV (212.8 nm). The arrow gives the laser polarization vector. Background electrons appear near the edge of the left edge of the image.

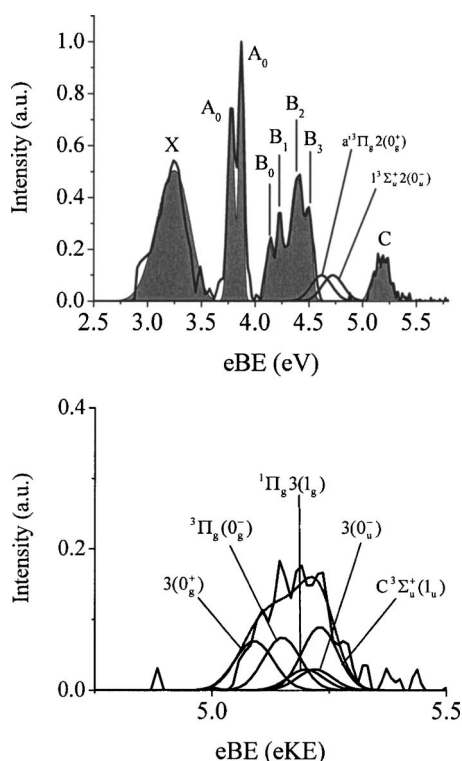


FIG. 5. Top: Photoelectron spectrum for I_2^- detached at 5.826 eV (212.8 nm). Assignments for bands are given in the text. The filled in area shows the FC simulation for the photoelectron spectrum. The simulations for photodetachment to the $a' \ ^3\Pi_u(2(0_g^+))$ state and the $1 \ ^3\Sigma_u^+(2(0_u^-))$ state are given in the figure. Bottom: We display the five excited states that fit the envelop for the C band in the photoelectron spectrum.

shows the I_2^- photoelectron spectrum obtained from the image in Fig. 4. The photoelectron spectrum is plotted in electron binding energy (eBE) defined as

$$eBE = h\nu - eKE,$$

where $h\nu$ is the energy of the detachment photon (5.826 eV for 212.8 nm) and eKE is the kinetic energy for the detached electron. The vertical detachment energy (VDE) is defined as the eBE at the band maximum.

From the transformed image, the photoelectron angular distribution is determined for each band and the angular distribution is fit according to²⁷

$$I(\theta) = \frac{1}{4\pi}(1 + \beta P_2(\cos \theta)),$$

where $I(\theta)$ is the photoelectron angular distribution and $P_2(\cos \theta)$ is the second Legendre polynomial. The anisotropy parameter β ranges from -1 to 2 , with the limits corresponding to $\sin^2 \theta$ and $\cos^2 \theta$ distributions, with respect to the laser polarization axis (arrow in Figs. 3 and 4).

The PE spectrum shown in Fig. 5 consists of four bands labeled X, A, B, and C. Bands X and C are broad and structureless while band A consists of two resolved peaks and band B consists of four partially resolved peaks. Table I gives the VDE and value of β for each band in the photoelectron spectrum. Our laboratory has previously observed bands X, A_0 , A_1 , B_0 , B_1 , and B_2 at lower photon energy with significantly higher resolution.^{11,13}

TABLE I. Vertical detachment energies.

| | β | VDE (eV) | Asmis <i>et al.</i> ^a | State assignment | Electronic configuration |
|-------|---------|----------|----------------------------------|---------------------------|--------------------------|
| X | 0.36 | 3.245 | 3.235 | $X \ ^1\Sigma_g^+(0_g^+)$ | 2440 |
| A_0 | -0.02 | 3.783 | 3.782 | $A' \ ^3\Pi_u(2_u)$ | 2431 |
| A_1 | -0.07 | 3.875 | 3.874 | $A \ ^3\Pi_u(1_u)$ | 2431 |
| B_0 | 0.08 | 4.134 | 4.124 | $B' \ ^3\Pi_u(0_u^-)$ | 2431 |
| B_1 | -0.01 | 4.240 | 4.235 | $B'' \ ^1\Pi_u(1_u)$ | 2341 |
| B_2 | 0.04 | 4.417 | 4.418* | $^3\Pi_g(2_g)$ | 2341 |
| | | | | $a \ ^3\Pi_g(1_g)$ | 2341 |
| B_3 | 0.11 | 4.503 | ... | $B \ ^3\Pi_u(0_u^+)$ | 2431 |
| C | -0.03 | 5.183 | ... | $3(0_g^+)$ | 2422 \rightarrow 2341 |
| | | | | $^3\Pi_g(0_g^-)$ | 2341 |
| | | | | $^1\Pi_g3(1_g)$ | 2341 |
| | | | | $3(0_u^-)$ | 2332 \rightarrow 1441 |
| | | | | $C \ ^3\Sigma_u^+(1_u)$ | 1441 |

^aReference 13.

Bands in the photoelectron spectra are assigned based on the previously calculated I_2^- ground state potential curve¹¹ and the curves for the ground and valence excited states of I_2 .³ The band assignments are given in Table I. Bands X and A were assigned previously as photodetachment to the $I_2 \ X \ ^1\Sigma_g^+(0_g^+)$ ground state, the $A' \ ^3\Pi_u(2_u)$, and the $A \ ^3\Pi_u(1_u)$ state.¹¹ Bands B_0 and B_1 have been assigned previously as photodetachment to the $B' \ ^3\Pi_u(0_u^-)$ and $B'' \ ^1\Pi_u(1_u)$ states, respectively.¹³ The assignments for bands B_2 , B_3 , and C require additional analysis, given in Sec. IV.

IV. ANALYSIS AND DISCUSSION

The photoelectron spectrum in Fig. 5 comprises transitions to multiple electronic states of I_2 , of which some are bound and others repulsive over the range of internuclear distances probed by photodetachment, the Franck-Condon (FC) region. Based on the potentials in Fig. 1 and our earlier photoelectron spectra, photodetachment to the X, A, A' , and B states accesses bound vibrational levels of I_2 , whereas transitions to the other electronic states primarily accesses continuum states. In simulations of the PE spectrum, these two types of transitions are treated somewhat differently. For the bound electronic states, the PE spectrum is simulated by calculating FC factors for transitions between anion and neutral vibrational levels. The resulting stick spectrum of individual vibrational transitions is then convoluted with the instrument resolution to generate the resulting band profile. Proper calculation of the FC factors requires the vibrational state distribution for the nascent anion, determined from an estimated temperature of 125 K. The equilibrium bond distances, R_e , the vibrational frequencies, ω_e , and the term energies, T_e , used in the FC simulations are from previous studies of I_2 (Table II). The parameters for I_2^- are from previous PE spectroscopy studies.^{11,13}

For electronic states in which photodetachment accesses the repulsive wall, we fit the neutral excited states³ to Morse potentials (typically with very shallow wells) and use the previously determined Morse function for the anion ground state.¹¹ Some of the adiabatic excited state curves for these neutral excited states undergo avoided crossings, but these

TABLE II. Parameters for I₂⁻ and I₂ from Franck-Condon simulations.

| | FC Simulation | | | Previous studies | | |
|---|---------------------|--------------------|------------------------------------|----------------------|----------------------|------------------------------------|
| | T _e (eV) | r _e (Å) | ω _e (cm ⁻¹) | T _e (eV) | r _e (Å) | ω _e (cm ⁻¹) |
| I ₂ (X) | ... | 3.205 | 110 | ... | 3.205 ^a | 110 ^a |
| | | | I ₂ | | | |
| X (¹ Σ _g ⁺) | 0 | 2.666 | 210 | 0 ^b | 2.666 ^b | 214 ^b |
| A' (³ Π _{2u}) | 1.241 | 3.079 | 109 | 1.245 ^c | 3.079 ^c | 109 ^c |
| | | | | (1.241) ^d | (3.123) ^d | (101) ^d |
| A (³ Π _{1u}) | 1.350 | 3.129 | 88 | 1.353 ^e | 3.129 ^e | 88 ^e |
| | | | | (1.351) ^d | (3.190) ^d | (85) ^d |
| B (³ Π _{0u} ⁺) | 1.950 | 3.024 | 115 | 1.955 ^f | 3.024 ^e | 126 ^e |
| | | | | (2.009) ^d | (3.070) ^d | (119) ^d |

^aReference 11.^bReferences 7 and 31.^cReference 32.^dReference 3.^eReference 33.^fReference 7.

occur at internuclear distances considerably shorter than those probed in our experiment;^{2,3} this point is considered in more detail below. Hence, Morse functions are an adequate representation of these curves in the anion FC region. The FC factors for transitions to the nominally repulsive states are determined using a discrete variable representation (DVR) procedure²⁸⁻³⁰ with an assumed anion vibrational temperature of 125 K.

The overall simulations are shown as gray shaded regions in Fig. 5. Band X has been previously observed and assigned as a transition to the I₂ X ¹Σ_g⁺(0_g⁺) ground electronic state.^{11,13} Photodetachment to the X ¹Σ_g⁺(0_g⁺) state corresponds to the 2441 → 2440 electronic transition, which is one-electron allowed. The large geometry change between the anion and neutral results in a photoelectron spectrum peaking at quantum numbers v' = 29–30 of the I₂ X ¹Σ_g⁺(0_g⁺), which accounts for the broad shape of this peak.¹¹ Using the well known experimental parameters for the anion and neutral ground states, the FC simulation fits band X with the adiabatic electron affinity of 2.524 ± 0.015 eV, in agreement with the literature value of 2.524 ± 0.005 eV.¹¹

Bands A₀ and A₁ were previously observed in the I₂⁻ photoelectron spectra at 299 nm and 266 nm.¹³ The two bands are fitted using the parameters in Table II for the A' ³Π_u(2_u) and A ³Π_u(1_u) state, respectively. Photodetachment to either state corresponds to a 2441 → 2431 electronic transition. The term energies for both bands lie within 4 meV of the previous experimental determinations. The 299 nm photoelectron spectrum from Zanni *et al.*¹¹ showed a limited vibrational progression for bands A₀ and A₁, but no progression are resolved for either band in Fig. 5.

We now discuss the analysis of bands B₀-B₃ and band C. In the previous study at 266 nm, bands B₀, B₁, and B₂ were observed and assigned to transitions to the B' ³Π_u(0_u⁻), B'' ¹Π_u(1_u), and B ³Π_u(0_u⁺) states of I₂, respectively, but no analysis was performed to support these assignments. At 266 nm, band B₃ was out of range. The more complete data set at 212.8 nm shows that the assignment of the band B₂ to the B ³Π_u(0_u⁺) was incorrect, and that band B₃ should be

assigned to this state. Photodetachment to the B ³Π_u(0_u⁺) state involves a 2441 → 2431 electronic transition. The FC simulation, using literature values⁷ for the term energy and the vibrational frequency, gives VDE = 4.509 eV for the B ³Π_u(0_u⁺) state, in good agreement with band B₃. The previous assignment of band B₂ peak as the B ³Π_u(0_u⁺) state yields a term energy almost 100 meV too low in energy and is therefore in error.

All remaining potential energy curves in Fig. 1 are repulsive in the FC region, although some of them have shallow wells (D_e ≤ 115 meV) with long equilibrium bond lengths (R_e > 3.7 Å). Hence, photodetachment will access continuum rather than bound states supported by these curves, and simulation of the corresponding bands B₀, B₁, B₂, and C in the photoelectron spectrum is done using the DVR code.

Band B₀ is fitted as the B' ³Π_u(0_u⁻) state, corresponding to a 2441 → 2431 electronic transition using the potential energy surface from de Jong *et al.*³ For the FC simulation, the term energy for the B' ³Π_u(0_u⁻) state is T_e = 1.514 ± 0.015 eV, in close agreement with the previous experimental number of 1.511 eV.⁵ Band B₁ is fitted using the potential for the B'' ¹Π_u(1_u) state of I₂ from de Jong *et al.*, corresponding to a 2441 → 2341 electronic transition³ with a term energy of T_e = 1.530 ± 0.015 eV in good agreement with the previous experimental value of 1.534 eV.⁶ These assignments agree with those given previously.¹³

Figure 1 shows that in the FC region of the anion (R = 3.205 Å), two very close-lying states lie between the B'' ¹Π_u(1_u) and the B ³Π_u(0_u⁺) states, namely, the ³Π_g(2_g) and a ³Π_g(1_g) states. Photodetachment to both states corresponds to a 2441 → 2341 electronic transition, so transitions to these states are reasonable candidates for band B₂. We find that band B₂ can be simulated using the potential energy surfaces calculated by de Jong *et al.*³ for the ³Π_g(2_g) and a ³Π_g(1_g) states without modification from Ref. 3. In the FC region, these states are split by only ~10 meV in the Franck-Condon region and we cannot resolve separate contributions from them, so we assume equal photodetachment cross sections.

Band C is quite broad (~300 meV) and its energy is in the range of photodetachment to several repulsive electronic states: the 3(0_g⁺) state (³Π_g in the FC region), ³Π_g(0_g⁻), and ¹Π_g3(1_g) states, all of which are predominantly 2341 in the FC region, and the 3(0_u⁻) state (³Σ_u⁺ in the FC region) and C ³Σ_u⁺(1_u) states, both of which are 1441 in the FC region. These states are shown by the orange curves in Fig. 1. With the exception of the C ³Σ_u⁺(1_u) state, none of the other four states contributing to band C have been experimentally observed. In order to fit the high energy edge of band C, the potential energy curve for the C ³Σ_u⁺(1_u) state in Ref. 3 had to be shifted down by 15 meV in the FC region of the anion. This is consistent with the observation by de Jong *et al.*³ that the calculated vertical excitation energy for the C ³Σ_u⁺(1_u) from the I₂ ground state is ~100 meV higher than the experimental value;³¹ the difference between the experimental and calculated curves should be smaller at larger R, since the asymptotic energy is fixed.

Note that the case (c) labels of these states refer to the

adiabatic potential energy curves, while the case (a) labels reflect the dominant character of each state in the anion FC region. According to de Jong *et al.*,³ there is an avoided crossing between the $3(0_g^+)$ and $2(0_u^+)$ states near $R_e(=2.666 \text{ \AA})$ for ground state I_2 , so that at the considerably longer internuclear distances ($\sim 3.2 \text{ \AA}$) probed by photodetachment, the dominant character of these two states is $^3\Pi_g$ (2341) and $^3\Sigma_g^-$ (2422), respectively, with only the first accessible by a one-electron transition; the case (a) and (*mnpq*) labels are reversed at $R < R_e$. Similarly, the $3(0_u^-)$ state has an avoided crossing with the $2(0_u^-)$ state at 2.78 \AA .^{2,3} Thus, in the the anion FC region, the dominant configuration of the $3(0_u^-)$ state is $^3\Sigma_u^+$ (1441), while that of the $2(0_u^-)$ state is mixed $^1\Sigma_u^-$, $^3\Sigma_u^+$ (2332).

The $2(0_g^+)$ and $2(0_u^-)$ states (magenta and green in Fig. 1) lie between the $B \ ^3\Pi_u(0_u^+)$ state and the $^3\Pi_g(0_g^-)$ states in the anion FC region and thus are energetically accessible. If photodetachment to either of these states occurred, we would observe additional features between the bands B_3 and C in the photoelectron spectrum, as shown by the lines in Fig. 5 (top). These simulated features do not match any of the experimental bands. The preceding discussion indicates that the dominant configurations of the $2(0_g^+)$ and $2(0_u^-)$ states in the anion FC region are 2422 and 2332, respectively; neither of which is accessible via one-electron detachment from the anion 2441 ground state. There are also several electronic states above the C state (dashed lines in Fig. 1) that are energetically accessible but not seen in our experiment. All have either 2422 or 2332 electronic character and are therefore not available through one-electron detachment. Hence, it appears that the relatively simple idea of one-electron detachment holds even for detachment to the fairly dense manifold of I_2 excited states probed in our experiment.

V. CONCLUSIONS

We have measured the photoelectron spectrum of I_2^- following detachment at 5.826 eV (212.8 nm) using VMI. The first three bands in the photoelectron spectrum, X , A_0 , and A_1 , have been observed in previous photoelectron experiments at 299 nm and 266 nm.¹¹ Band X is fitted as I_2^- photodetachment to $I_2 X \ ^1\Sigma_g^+(0_g^+)$ and bands A_0 and A_1 as photodetachment to $I_2 A' \ ^3\Pi_u(2_u)$ and $I_2 A \ ^3\Pi_u(1_u)$ using a FC simulation. Bands B_0 and B_1 in the photoelectron spectrum were observed previously at 4.661 eV detachment energy and assigned as transitions to the $B' \ ^3\Pi_u(0_u^-)$ and $B'' \ ^1\Pi_u(1_u)$ states of I_2 , respectively. The previous I_2^- photoelectron study at 4.661 eV assigned band B_2 as photodetachment to $I_2 B \ ^3\Pi_u(0_u^+)$. According to the Franck-Condon simulations the vertical detachment energy for $I_2 B \ ^3\Pi_u(0_u^+)$ is 4.509 eV which is in good agreement with band B_3 . Band B_2 is reassigned as photodetachment to the repulsive walls of the $^3\Pi_g(2_g)$ and $a \ ^3\Pi_g(1_g)$ excited states of I_2 . Band C is assigned as photodetachment to a series of I_2 repulsive states: $^3\Sigma_g^-3(0_g^+)$, $^3\Pi_g2(0_g^-)$, $^1\Pi_g3(1_g)$, $^1\Sigma_u^-3(0_u^-)$, and $C \ ^3\Sigma_u^+(1_u)$. Finally, transitions to several excited states of I_2 do not appear in the photoelectron spectrum. The missing transitions corre-

spond to photodetachment to excited states involving a two-electron change in orbital occupancy, which is nominally forbidden.

ACKNOWLEDGMENTS

This research is supported by the National Science Foundation under Grant No. DMR-0505311. The authors thank Dr. de Jong for providing the potential energy surfaces for I_2 , which we used for DVR simulation. One of the authors (K.E.K.) acknowledges a NSF Graduate Research Fellowship and a Chancellors Predoctoral Opportunity Fellowship from the University of California.

- ¹R. S. Mulliken, *J. Chem. Phys.* **55**, 288 (1971).
- ²C. Teichteil and M. Pelissier, *Chem. Phys.* **180**, 1 (1994).
- ³W. C. de Jong, L. Visscher, and W. C. Nieuwpoort, *J. Chem. Phys.* **107**, 9046 (1997).
- ⁴J. Tellinghuisen, *J. Chem. Phys.* **76**, 4736 (1982).
- ⁵K. S. Viswanathan and J. Tellinghuisen, *J. Mol. Spectrosc.* **101**, 285 (1983).
- ⁶J. Tellinghuisen, *J. Chem. Phys.* **82**, 4012 (1985).
- ⁷F. Martin, R. Bacis, S. Churassy, and J. Verges, *J. Mol. Spectrosc.* **116**, 71 (1986).
- ⁸A. Zaitsevskii, E. A. Pazyuk, A. V. Stolyarov, C. Tiechteil, and V. Vallet, *Mol. Phys.* **98**, 1973 (2000).
- ⁹J. Vala, R. Kosloff, and J. N. Harvey, *J. Chem. Phys.* **114**, 7413 (2001).
- ¹⁰J. C. D. Brand and A. R. Hoy, in *Applied Spectroscopy Reviews*, edited by E. G. Brame, Jr. (Dekker, New York, 1987), Vol. 23, pp. 285.
- ¹¹M. T. Zanni, T. R. Taylor, B. J. Greenblatt, B. Soep, and D. M. Neumark, *J. Chem. Phys.* **107**, 7613 (1997).
- ¹²O. Fossgaard, O. Gropen, M. C. Valero, and T. Saue, *J. Chem. Phys.* **118**, 10418 (2003).
- ¹³K. R. Asmis, T. R. Taylor, C. Xu, and D. M. Neumark, *J. Chem. Phys.* **109**, 4389 (1998).
- ¹⁴B. J. Greenblatt, M. T. Zanni, and D. M. Neumark, *Chem. Phys. Lett.* **258**, 523 (1996).
- ¹⁵M. T. Zanni, V. S. Batista, B. J. Greenblatt, W. H. Miller, and D. M. Neumark, *J. Chem. Phys.* **110**, 3748 (1999).
- ¹⁶R. Mabbs, K. Pichugin, and A. Sanov, *J. Chem. Phys.* **122**, 174305 (2005).
- ¹⁷B. Baguenard, J. B. Wills, F. Pagliarulo, F. Lepine, B. Climen, M. Barbaire, C. Clavier, M. A. Lebeault, and C. Bordas, *Rev. Sci. Instrum.* **75**, 324 (2004).
- ¹⁸S. M. Sheehan, G. Meloni, B. F. Parsons, N. Wehres, and D. M. Neumark, *J. Chem. Phys.* **124**, 064303 (2006).
- ¹⁹G. J. Rathbone, T. Sanford, D. Andrews, and W. C. Lineberger, *Chem. Phys. Lett.* **40**, 570 (2005).
- ²⁰L. A. Posey, M. J. Deluca, and M. A. Johnson, *Chem. Phys. Lett.* **131**, 170 (1986).
- ²¹R. B. Metz, T. Kitsopoulos, A. Weaver, and D. M. Neumark, *J. Chem. Phys.* **88**, 1463 (1988).
- ²²O. Cheshnovsky, S. H. Yang, C. L. Pettiette, M. J. Craycraft, and R. E. Smalley, *Rev. Sci. Instrum.* **58**, 2131 (1987).
- ²³D. Proch and T. Trickl, *Rev. Sci. Instrum.* **60**, 713 (1989).
- ²⁴D. W. Chandler and P. L. Houston, *J. Chem. Phys.* **87**, 1445 (1987).
- ²⁵A. T. J. B. Eppink and D. H. Parker, *Rev. Sci. Instrum.* **68**, 3477 (1997).
- ²⁶V. Dribinski, A. Ossadtchi, V. A. Mandelshtam, and H. Reisler, *Rev. Sci. Instrum.* **73**, 2634 (2002).
- ²⁷J. Cooper and R. N. Zare, *Rev. Sci. Instrum.* **48**, 942 (1968).
- ²⁸Z. Bacic and J. C. Light, *Annu. Rev. Phys. Chem.* **40**, 469 (1989).
- ²⁹J. C. Light, I. P. Hamilton, and J. V. Lill, *J. Chem. Phys.* **82**, 1400 (1985).
- ³⁰R. B. Metz, A. Weaver, S. E. Bradforth, T. N. Kitsopoulos, and D. M. Neumark, *J. Phys. Chem.* **94**, 1377 (1990).
- ³¹K. P. Huber and G. Herzberg, *Constants of Diatomic Molecules* (van Nostrand Reinhold, New York, 1979).
- ³²J. B. Koffend, A. M. Sibai, and R. Bacis, *J. Phys. (Paris)* **43**, 1639 (1982).
- ³³S. Gesternkorn, P. Luc, and J. Verges, *J. Phys. B* **14**, L193 (1981).